



Original Article

## Frictional forces in stent retriever procedures: The impact of vessel diameter, angulation, and deployment position

Kazuma Tsuto<sup>1</sup>, Masataka Takeuchi<sup>2</sup> , Yu Shimizu<sup>2</sup>, Takashi Matsumoto<sup>2</sup>, Satoshi Iwabuchi<sup>3</sup>

<sup>1</sup>Department of Neurosurgery, Toho University Graduate School of Medicine, Meguroku, <sup>2</sup>Department of Neurosurgery, Seisho Hospital, Odawara,

<sup>3</sup>Department of Neurosurgery, Toho University Ohashi Medical Center, Meguroku, Japan.

E-mail: \*Kazuma Tsuto - ktsuto17@gmail.com; Masataka Takeuchi - masatakatakeuchi@hotmail.com; Yu Shimizu - bleuler3a@yahoo.co.jp; Takashi Matsumoto - tktkjp84@gmail.com; Satoshi Iwabuchi - iwabuchi@med.toho-u.ac.jp



\*Corresponding author:

Kazuma Tsuto,  
Department of Neurosurgery,  
Toho University Graduate  
School of Medicine, Meguroku,  
Japan.

ktsuto17@gmail.com

Received: 19 August 2024

Accepted: 21 September 2024

Published: 25 October 2024

DOI

10.25259/SNI\_709\_2024

Quick Response Code:



### ABSTRACT

**Background:** Mechanical thrombectomy has improved the outcome of patients with acute ischemic stroke, but complications such as subarachnoid hemorrhage (SAH) can worsen the prognosis. This study investigates the frictional forces exerted by stent retrievers (SRs) on vessel walls, hypothesizing that these forces contribute to vascular stress and a risk of hemorrhage. We aimed to understand how vessel diameter, curvature, and stent deployment position influence these forces.

**Methods:** Using a silicone vascular model simulating the middle cerebral artery, we created virtual vessels with diameters of 2.0 mm and 2.5 mm, each with branching angles of 60° and 120°. A Trevo NXT (4 × 28 mm) SR was deployed and retracted through these models, measuring the maximum static frictional force at the moment the SR began to move. The stent deployment position relative to the curvature (straight, distal 1/4, center, and proximal 1/4) was also varied to assess its impact on frictional forces. Each condition was tested 15 times, and the results were statistically analyzed.

**Results:** The highest frictional force was observed in the 2.0 mm/120° model, followed by the 2.0 mm/60°, 2.5 mm/120°, and 2.5 mm/60° models. Narrower and more sharply curved vessels exhibited significantly higher frictional forces. Friction also increased with more distal stent deployment, particularly in the narrower vessels.

**Conclusion:** Smaller vessel diameters, greater curvature, and more distal stent deployment positions increase frictional forces during thrombectomy, potentially leading to SAH. These findings highlight the importance of selecting appropriately sized SRs and considering stent deployment positions to minimize vascular stress.

**Keywords:** Frictional forces, Mechanical thrombectomy, Stent retrievers, Vascular curvature, Vessel diameter

### INTRODUCTION

In recent years, remarkable progress in mechanical thrombectomy for acute cerebral vessel occlusion has led to improved outcomes in ischemic stroke treatment. However, hemorrhagic complications during thrombectomy can adversely affect patient prognosis.<sup>[6,7,11,12]</sup> Asymptomatic intracranial hemorrhage, even when detected solely by a computed tomography (CT) scan immediately after a procedure without any accompanying neurological symptoms, is still considered a predictor of poor outcomes.<sup>[5,8,25,26]</sup> Achieving recanalization while minimizing hemorrhagic complications is essential. Although subarachnoid hemorrhage (SAH) is occasionally observed on head CT after thrombectomy,<sup>[2,21,28]</sup> the exact mechanisms remain

This is an open-access article distributed under the terms of the Creative Commons Attribution-Non Commercial-Share Alike 4.0 License, which allows others to remix, transform, and build upon the work non-commercially, as long as the author is credited and the new creations are licensed under the identical terms.

©2024 Published by Scientific Scholar on behalf of Surgical Neurology International

unclear. When traction is applied to the delivery wire, significant vessel deviation can occur, particularly before the stent retriever (SR) begins to move. It has been suggested that this vessel deviation may cause tears in small branches, leading to bleeding.<sup>[20,29]</sup> There is also a possibility that pulling the SR could damage the vessel wall, potentially causing dissection or perforation.<sup>[19]</sup> Therefore, approaches that reduce vessel stress as much as possible are required. In this study, we hypothesized that the maximum static frictional force exerted on the vessel wall when the SR begins to move represents the force responsible for vessel deviation and the resulting stress on the vessel wall in clinical practice. We measured how this force varies based on two factors: “vessel diameter” and “branching angle” using a vascular model.

## MATERIALS AND METHODS

A cylindrical cavity was created in a plate-shaped silicone material to simulate virtual blood vessels, specifically modeling the middle cerebral artery's (MCA) M1 and M2 segments based on several clinical studies.<sup>[15,18]</sup> Two types of virtual blood vessels were fabricated with inner diameters of 2.0 mm and 2.5 mm, respectively. Each vessel model incorporated central angles of 60° and 120°, resulting in four different comparable conditions [Figure 1]. These vascular models were placed in

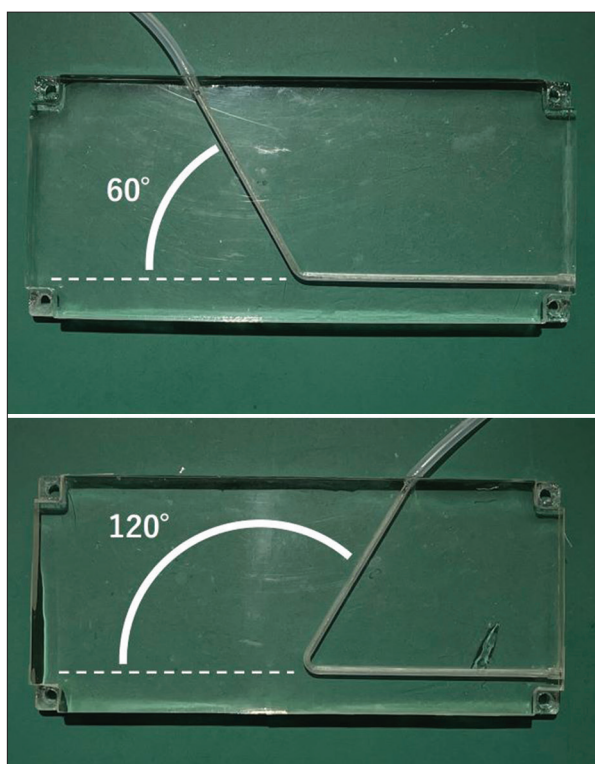


**Figure 1:** A virtual vascular model, created by forming a cylindrical cavity in a plate-shaped silicon material, features inner diameters of 2.0 and 2.5 mm with bends of 60° and 120°, respectively.

containers filled with surfactant at 37°C, with their lumens also filled with surfactant. A guiding catheter was inserted into the lumen, and a microcatheter was passed through the bend [Figure 2a]. A trevo NXT (4 × 28 mm, Stryker, Kalamazoo, Michigan, USA) was then deployed through the microcatheter, ensuring the bend aligned with the proximal 1/4 of the stent [Figure 2b]. The deployment process was monitored visually using a fixed-position miniature camera, and the position of the stent's distal end was marked on a monitor to ensure consistent deployment for each procedure [Figure 2c].

A traction device was attached to the delivery wire of the deployed SR, and linear traction was applied at a speed of 1 cm per second [Figures 2d and e]. The pulling load was recorded at a rate of 100 data points per second using a digital indicator. The maximum static friction force encountered when the SR began to move was assumed to represent the burden on the vessel in clinical practice and was calculated under four conditions. Three Trevo SRs were used for each condition, and each Trevo underwent this traction procedure 5 times. A total of 15 SR tractions were performed for each condition, and the mean values were compared across the four conditions. Furthermore, using the traction force of the Trevo retriever in a straight 2.0 mm lumen as a reference, the changes in traction force were analyzed based on the deployment position of the SR relative to the bend (proximal 1/4, central, distal 1/4) under the condition expected to produce the highest static friction force (2.0 mm/120°).

## Statistical analysis

Statistical differences were analyzed using Bartlett's test to assess the homogeneity of variances across groups. If the variances were equal, a one-way analysis of variance (ANOVA) was conducted; if they were unequal, the Kruskal–Wallis test was used. Multiple comparisons were performed using Tukey's *post hoc* test following ANOVA and the Steel–Dwass method following the Kruskal–Wallis test. A  $P < 0.05$  was considered statistically significant. All statistical analyses were conducted using Statcel, an Excel add-in (4<sup>th</sup> edition).

## RESULTS

In all procedures, peak load on the traction device was observed at the moment the SR began to move. Figure 3 illustrates the results of the retrieval experiment using the traction device [Figure 3].

The maximum static friction force exerted when the SR began to move was highest in the vessel with a 2.0 mm diameter and a 120° curvature (mean ± standard deviation: 60.7 ± 9.0 g), followed by the 2.0 mm/60° (44.4 ± 9.1 g), the 2.5 mm/120° (40.4 ± 6.0 g), and the 2.5 mm/60° (36.8 ± 6.6 g) conditions, in that order. Significant differences were observed among these four groups (one-way ANOVA;  $P < 0.01$ ). Pairwise

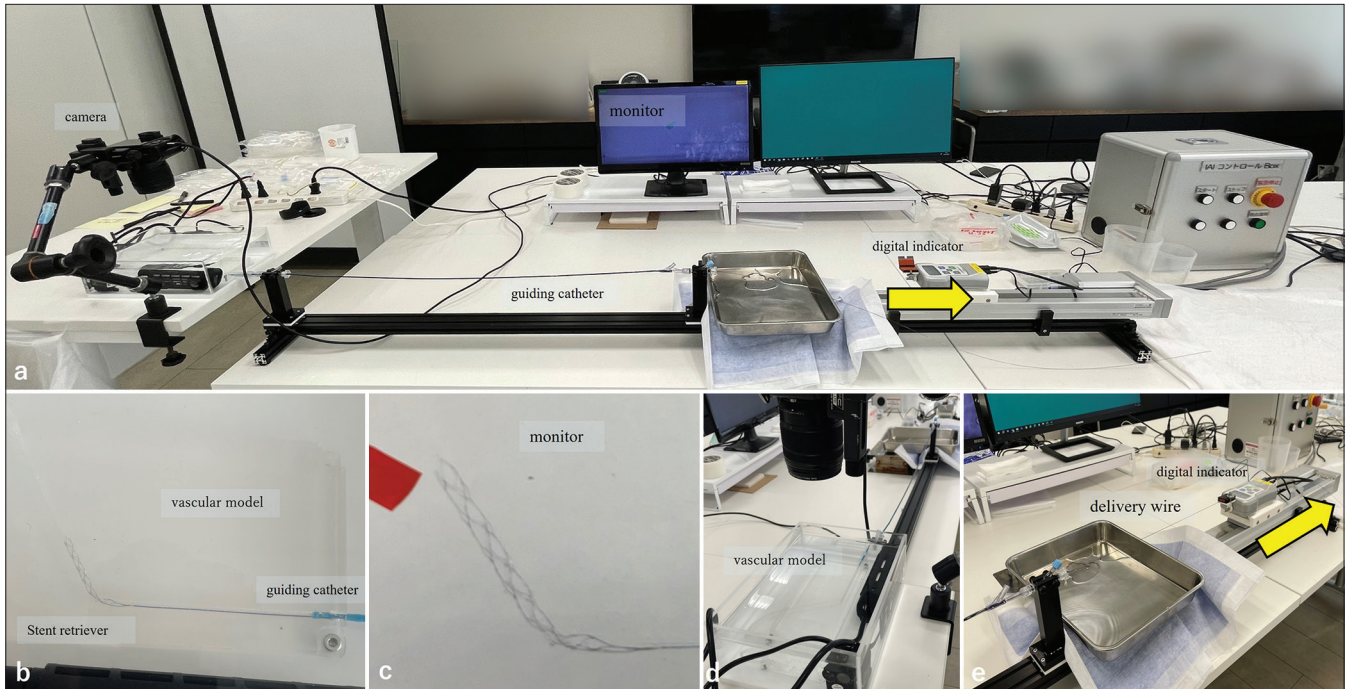


**Figure 2:** An experimental model for measuring stent retrieval frictional force. (a) Overview of the model. (b) The stent retriever is deployed within the vascular model filled with 37°C surfactant. (c) To ensure consistent stent deployment positions, the vascular model was captured on camera, and the position of the stent’s distal end was marked on an enlarged monitor. (d) The delivery wire of the stent was passed through the guiding catheter. (e) The proximal end of the delivery wire was fixed to a gripper attached to a digital indicator. The yellow arrows indicate the action of traction applied by the traction device.

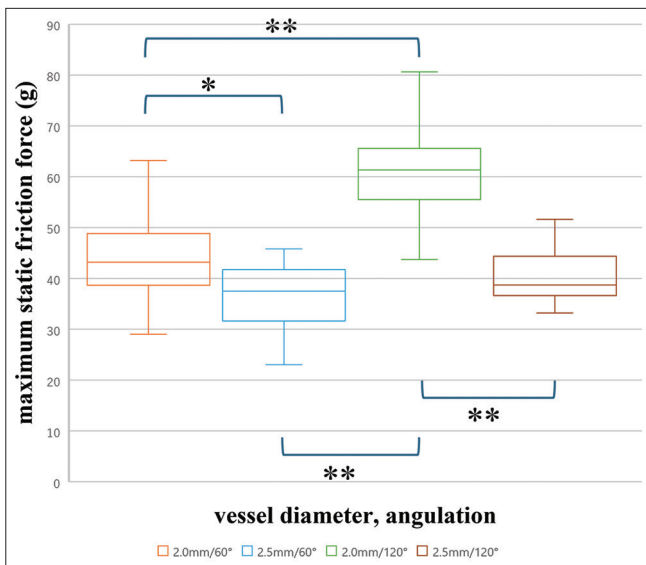


**Figure 3:** Comparison of friction force during stent pulling among four conditions. In a one-way analysis of variance with Tukey’s *post hoc* test, \*\* $P < 0.01$ , \* $P < 0.05$ .

comparisons revealed that in vessels with a smaller diameter (2.0 mm), a greater curvature resulted in a significantly higher friction force. Conversely, in vessels with a larger diameter (2.5 mm), increasing the curvature did not lead

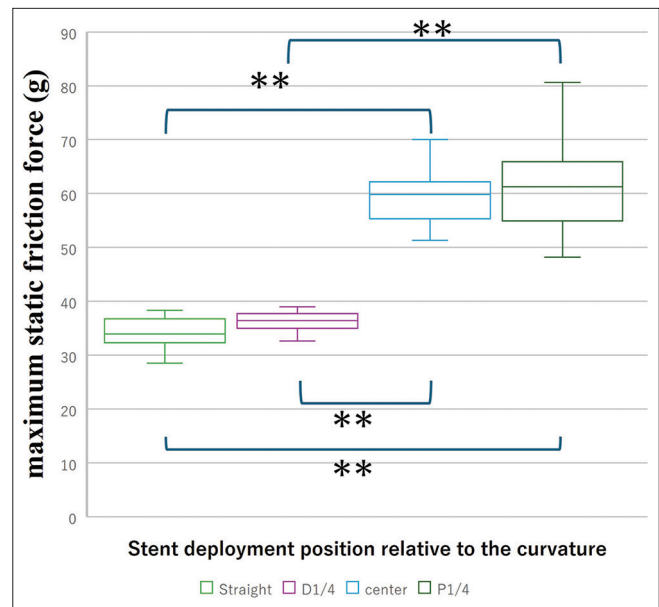


**Figure 4:** Comparison of maximum static friction force among different stent deployment positions relative to the curvature. The box plots illustrate the frictional forces measured when the stent is deployed in various positions: straight, distal 1/4 (D1/4), center, and proximal 1/4 (P1/4) relative to the curvature. In the Kruskal–Wallis test with the Steel–Dwass method, \*\* $P < 0.01$ .

to significant differences in friction force (Tukey–Kramer method). Furthermore, the maximum static friction force in the straight section of the 2.0 mm lumen model was  $34.2 \pm 3.0$  g. Significant differences were observed among the four conditions where the stent deployment position varied relative to the curved section, with a tendency for stronger traction forces as the deployment position moved more distally (Kruskal–Wallis test) [Figure 4].

However, in comparisons among the groups, no significant differences in traction forces were found between the group where the stent was deployed in the straight section and the group where the distal 1/4 of the stent was positioned in the curved area ( $36.4 \pm 2.6$  g). Similarly, no significant differences were found between the group where the central portion of the stent was aligned with the curved section ( $59.4 \pm 4.9$  g) and the group where the proximal 1/4 was positioned in the same area (Steel–Dwass method).

## DISCUSSION

When thrombectomy using SRs is performed for occlusions in the distal MCA, the recanalization rate is generally high. However, SAH is reported to occur more frequently compared to occlusions in the proximal MCA or internal carotid artery (ICA).<sup>[9,14,23]</sup> As a result, large-scale randomized controlled trials have not been conducted, and the effectiveness of this procedure has not been proven at this time. Consequently, the detailed mechanism underlying SAH following thrombectomy remains unclear. One possible cause is the stretching of arterioles and accompanying venules in the subarachnoid space due to the displacement of blood vessels during SR withdrawal.<sup>[17]</sup> The basis for this is the localization of SAHs in the ipsilateral Sylvian fissure near the path of the occluded MCA<sup>[29]</sup> and the exacerbation of this phenomenon due to the length of the SR positioned along the M2 branch.<sup>[19]</sup> The stretching of blood vessels results from the friction between the SR and the vessel wall, with the greatest stress occurring at the moment the SR begins to move.

In our experiment, we hypothesized that the maximum static friction force applied to the traction device at the moment the SR starts to move corresponds to the force that causes vascular displacement.

This study is the first to investigate how vascular diameter and curvature affect frictional forces between an SR and the vessel using a vascular model. Machi *et al.*, similarly demonstrated that greater friction occurs when withdrawing an SR within a narrower tube<sup>[16]</sup>, but they did not investigate the effects of varying degrees of angulation. Our primary finding shows that in thrombectomy with the same SR, the stress on narrower blood vessels is significantly greater. In addition, while sharp angles do not increase vessel stress if the vascular diameter is large, stress increases with greater angulation when the

diameter is small. These findings suggest that such factors could influence the incidence of complications in clinical practice. Along with removing thrombi and restoring vessel patency, one of the aims of mechanical thrombectomy is also to reduce postoperative bleeding complications. The *in vitro* results suggest that selecting an SR appropriate for the vascular diameter may help reduce the incidence of SAH. Furthermore, special caution is required when using an SR in narrow and highly angulated vessels. In fact, Kim *et al.* retrospectively reviewed cases of mechanical thrombectomy for M2 occlusion and found that sulcal SAH was observed more frequently in cases involving distal vessel occlusion or greater angulation of bifurcations,<sup>[10]</sup> corroborating our findings in clinical practice. In general, in cases of acute vessel occlusion, the vessel diameter and course beyond the occluded site could be unknown. Therefore, it is advisable to select the optimal SR that minimizes the burden on the vessel based on the angiography from the microcatheter passed beyond the occluded site or the degree of bending of the microcatheter itself.

Another concern when using an SR in cerebral blood vessels is the potential for vascular damage during the retrieval process. Shibata *et al.* reported a case of vessel perforation during thrombectomy with a 6-mm SR in a single pass for tandem occlusion of the ICA and distal M1,<sup>[24]</sup> highlighting that vessel perforation can occur even with a single pass if the appropriate SR size for the vessel diameter is not selected. Teng *et al.* reported using an *in vitro* live cell artificial vessel system, where smaller vessel diameters resulted in greater endothelial cell injury,<sup>[27]</sup> suggesting the importance of selecting devices that properly match the vessel dimensions. In addition to these findings, our study demonstrated that when the size of the SR is not suited to the vessel diameter, greater curvature results in significantly higher static friction forces. Naturally, M2 vessels are narrower and more curved compared to M1 vessels, which likely contributes to the higher incidence of vessel injury and

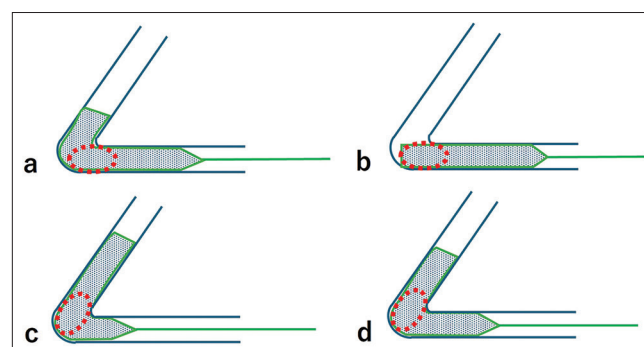


**Figure 5:** Illustration showing the differences in stent deployment positions relative to the curved section of a blood vessel. (a) Stent deployed in the straight section, (b-d) Stent deployed with different sections (distal 1/4, center, proximal 1/4) aligned with the curve. The red circles indicate the location of the thrombus.

postoperative SAH reported in multiple studies involving M2 vessels.<sup>[1,14,22]</sup> Hence, these findings suggest that in cases of distal vessel occlusion with high curvature, it is crucial to select an SR that appropriately matches the size of the vessel to minimize the risk of vascular damage.

In the SR procedure, it is important to minimize the burden on the vessel, as well as to maximize the probability of successful reperfusion. Achieving both goals may require careful consideration of the stent's deployment position relative to the vessel's curvature. To enhance thrombus capture by the stent struts, the stent should be deployed more distally relative to the thrombus. However, Funatsu *et al.* reported that when the SR was positioned more distally, it often encountered vascular wall components within the thrombus,<sup>[3]</sup> indicating a higher risk of vessel injury during thrombus retrieval. Our study corroborates this finding, demonstrating that stronger friction forces occur when the stent is deployed more distally relative to the curved section of the vessel. Figure 5 shows the differences in stent deployment positions relative to the curved section [Figure 5]. Interestingly, deploying the distal 1/4 of the stent over the curved section [Figure 5a] did not significantly increase the burden on the vessel during retrieval compared to deployment in the straight section [Figure 5b]. This suggests that when the thrombus is located just proximal to the curved section, deploying the stent more distally, slightly over the curved section, can improve retrieval efficiency without significantly increasing vessel stress. Similarly, no additional vessel burden was observed when deploying the proximal quarter [Figure 5c] or the central portion [Figure 5d] of the stent over the curved section. This suggests that when the thrombus is just distal to the curved section, deploying the stent more distally might enhance retrieval efficiency. In contrast to this experiment, of course, it is often difficult to have enough information to determine the location and length of the thrombus preoperatively in cases of acute vessel occlusion. Nevertheless, if these factors can be identified using the susceptibility vessel sign on magnetic resonance imaging T2\* sequence or through simultaneous contrast media injection from both the microcatheter and guiding catheter,<sup>[19]</sup> the techniques mentioned above could potentially improve retrieval efficacy.

To better understand how SRs function in the human cerebral artery, a model that closely resembles the actual vascular environment is required. Kwak *et al.* developed a cerebral artery model using 3D printing based on real human cerebral angiograms.<sup>[13]</sup> To replicate the elasticity of real vessels, they used multilayer coatings of silicone elastomer-hydrogel with an inner hydrogel coating to simulate the lubrication provided by the endothelium. A pulsatile blood pump was employed to simulate blood flow. They reported variations in frictional forces among different SRs under these conditions. However, they did not explore the differences in frictional

forces due to the angle of vascular curvature or the vascular diameter. We focused on these two factors to investigate their influence on vessel stress. Our findings indicated that when using the same SR, vascular diameter contributed more to the increase in frictional force than vascular angle.

Our study has certain limitations. First, it is an *in vitro* study using a rigid silicone model, which means that the vessels did not deform as they would in real-life conditions. In actual thrombectomy procedures within human cerebral arteries, vessels are expected to deform during SR retrieval, and our study could not assess the extent to which this deformation contributes to vessel stress. The accordion-like shortening along the longitudinal axis, often observed in real cerebral vessels, is difficult to replicate. Second, as previously mentioned, various factors such as vessel elasticity, endothelial characteristics, blood flow, number of bends, and properties and length of the thrombus play a role in the clinical environment.<sup>[4,16]</sup> Accurately determining how these factors relate to real-world scenarios based solely on the results of this experiment is difficult. To address these issues, further experiments using models more similar to human cerebral arteries are needed.

## CONCLUSION

Our study findings show that frictional forces exerted by SRs on vessel walls are significantly influenced by vessel diameter, curvature, and stent deployment position. Smaller diameters, greater curvature, and more distal stent deployment result in higher frictional forces during thrombectomy, potentially increasing to the risk of hemorrhagic complications such as SAH. These findings highlight the necessity of selecting SRs appropriately sized for the vessel and carefully considering deployment position to minimize vascular stress. Future studies with models that better replicate human cerebral arteries are essential to further validate these results and optimize thrombectomy techniques.

## Ethical approval

Institutional Review Board approval is not required as this study did not involve human subjects and presented results from experimental models; therefore, we determined that ethical approval was not required, and this was confirmed by the ethics committee of our institution.

## Declaration of patient consent

Patient's consent is not required as there are no patients in this study.

## Financial support and sponsorship

The study was financially supported by Kaneka Medix.

## Conflicts of interest

There are no conflicts of interest.

## Use of artificial intelligence (AI)-assisted technology for manuscript preparation

The authors confirm that there was no use of artificial intelligence (AI)-assisted technology for assisting in the writing or editing of the manuscript and no images were manipulated using AI.

## REFERENCES

- Baharvahdat H, Ooi YC, Khatibi K, Ponce Mejia LL, Kaneko N, Nour M, *et al.* Increased rate of successful first passage recanalization during mechanical thrombectomy for M2 occlusion. *World Neurosurg* 2020;139:e792-e9.
- Charbonnier G, Bonnet L, Biondi A, Moulin A. Intracranial bleeding after reperfusion therapy in acute ischemic stroke. *Front Neurol* 2021;11:629920.
- Funatsu N, Hayakawa M, Hashimoto T, Yamagami H, Satow T, Takahashi, JC, *et al.* Vascular wall components in thrombi obtained by acute stroke thrombectomy: Clinical significance and related factors. *J Neurointerv Surg* 2019;11:232-6.
- Gunning GM, MacArdle K, Mirza M, Duffy S, Gilvarry M, Brouwer PA. Clot friction variation with fibrin content; implications for resistance to thrombectomy. *J Neurointerv Surg* 2018;10:34-8.
- Harker P, Aziz YN, Vranic J, Chulluncuy-Rivas R, Previtera M, Yaghi S, *et al.* Asymptomatic intracerebral hemorrhage following endovascular stroke therapy is not benign: A systematic review and meta-analysis. *J Am Heart Assoc* 2024;13:e031749.
- Hao Y, Yang D, Wang H, Zi W, Zhang M, Geng Y, *et al.* Predictors for symptomatic intracranial hemorrhage after endovascular treatment of acute ischemic stroke. *Stroke* 2017;48:1203-9.
- He J, Fu F, Zhang W, Zhan Z, Cheng Z. Prognostic significance of the clinical and radiological haemorrhagic transformation subtypes in acute ischaemic stroke: A systematic review and meta-analysis. *J Neurol* 2022;29:3449-59.
- Jiang F, Zhao W, Wu C, Zhang Z, Li C, Che R, *et al.* Asymptomatic intracerebral hemorrhage may worsen clinical outcomes in acute ischemic stroke patients undergoing thrombectomy. *J Stroke Cerebrovasc Dis* 2019;28:1752-8.
- Jumma MA, Castonguay AC, Salahuddin H, Jadhav AP, Limaye K, Farooqui M, *et al.* Middle cerebral artery M2 thrombectomy in the STRATIS Registry. *Stroke* 2021;52:3490-6.
- Kim DY, Baik SH, Jung C, Kim JY, Han SG, Kim BJ, *et al.* Predictors and impact of sulcal SAH after mechanical thrombectomy in patients with isolated M2 occlusion. *Am J Neuroradiol* 2022;43:1292-8.
- Kinjo N, Yoshimura S, Uchida K, Sakai N, Yamagami H, Morimoto T, *et al.* Incidence and prognostic impact of intracranial hemorrhage after endovascular treatment for acute large vessel occlusion. *Cerebrovasc Dis* 2020;49:540-9.
- Knief H, Meyer L, Brooks G, Bechstein M, Guerreiro H, Winkelmeier L, *et al.* Predictors of functional outcome after thrombectomy for M2 occlusions: A large scale experience from clinical practice. *Sci Rep* 2023;13:18740.
- Kwak Y, Son W, Kim BJ, Kim M, Yoon SY, Park J, *et al.* Frictional force analysis of stent retriever devices using a realistic vascular model: Pilot study. *Front Neurol* 2022;13:964354.
- Lee H, Qureshi AM, Mueller-Kronast NH, Zaidat OO, Froehler MT, Liebeskind DS, *et al.* Subarachnoid hemorrhage in mechanical thrombectomy for acute ischemic stroke: Analysis of the STRATIS registry, systematic review and meta-analysis. *Front Neurol* 2021;12:663058.
- Liu D, Zhang G, Wang Y, Li J, Cao P, Yin X, *et al.* Geometric features of middle cerebral artery are associated with spontaneous basal ganglia intracerebral haemorrhage. *Stroke Vasc Neurol* 2022;7:399-405.
- Machi P, Jourdan F, Ambard D, Reynaud C, Lobotesis K, Sanchez M, *et al.* Experimental evaluation of stent retrievers' mechanical properties and effectiveness. *J Neurointerv Surg* 2017;9:257-63.
- Mokin M, Fargen KM, Primiani CT, Ren Z, Dumont TM, Brasiliense LB, *et al.* Vessel perforation during stent retriever thrombectomy for acute ischemic stroke: Technical details and clinical outcomes. *J Neurointerv Surg* 2017;9:922-8.
- Mouches P, Forkert ND. A statistical atlas of cerebral arteries generated using multi-center MRA datasets from healthy subjects. *Sci Data* 2019;6:29.
- Naggara O, Raymond J, Domingo M, Al-Shareef F, Touzé E, Chenoufi M, *et al.* T2\* "susceptibility vessel sign" demonstrates clot location and length in acute ischemic stroke. *PLoS One* 2013;8:e76727.
- Ng PP, Larson TC, Nichols CW, Murray MM, Salzman KL, Smith RH. Intraprocedural predictors of post-stent retriever thrombectomy subarachnoid hemorrhage in middle cerebral artery stroke. *J Neurointerv Surg* 2019;11:127-32.
- Nikoubashman O, Reich A, Pjontek R, Jungbluth M, Wiesmann M. Postinterventional subarachnoid haemorrhage after endovascular stroke treatment with stent retrievers. *Neuroradiology* 2014;56:1087-96.
- Nome T, Enriquez B, Nome CG, Tennøe B, Lund CG, Skjelland M, *et al.* Clinical outcome after thrombectomy in patients with MeVO stroke: Importance of clinical and technical factors. *J Neurointerv Surg* 2024;271:877-86.
- Renieri L, Valente I, Dmytriw AA, Puri AS, Singh J, Nappini S, *et al.* Mechanical thrombectomy beyond the circle of Willis: Efficacy and safety of different techniques for M2 occlusions. *J Neurointerv Surg* 2022;14:546-50.
- Shibata A, Yanagawa T, Sugasawa S, Ikeda S, Ikeda T. Multiple large vessel occlusions resulting in vessel perforation in single pass of mechanical thrombectomy with stent retriever. *Radiol Case Rep* 2023;18:3206-11.
- Suzuki K, Katano T, Numao S, Nishi Y, Kutsuna A, Kanamaru T, *et al.* The effect of asymptomatic intracranial hemorrhage after mechanical thrombectomy on clinical outcome. *J Neurol Sci* 2024;457:122868.
- Tang G, Cao Z, Luo Y, Wu S, Sun X. Prognosis associated with asymptomatic intracranial hemorrhage after acute ischemic stroke: A systematic review and meta-analysis. *J Neurol* 2022;269:3470-81.

27. Teng D, Pannell JS, Rennert RC, Li J, Li YS, Wong VW, *et al.* Endothelial trauma from mechanical thrombectomy in acute stroke: *In vitro* live-cell platform with animal validation. *Stroke* 2015;46:1099-106.
28. Yilmaz U, Walter S, Körner H, Papanagiotou P, Roth C, Simgen A, *et al.* Peri-interventional subarachnoid hemorrhage during mechanical thrombectomy with stent retrievers in acute stroke: A retrospective case-control study. *Clin Neuroradiol* 2015;25:173-6.
29. Yoon W, Jung MY, Jung SH, Park MS, Kim JT, Kang HK. Subarachnoid hemorrhage in a multimodal approach heavily weighted toward mechanical thrombectomy with solitaire stent in acute stroke. *Stroke* 2013;44:414-9.

**How to cite this article:** Tsuto K, Takeuchi M, Shimizu Y, Matsumoto T, Iwabuchi S. Frictional forces in stent retriever procedures: The impact of vessel diameter, angulation, and deployment position. *Surg Neurol Int.* 2024;15:384. doi: 10.25259/SNI\_709\_2024

### Disclaimer

The views and opinions expressed in this article are those of the authors and do not necessarily reflect the official policy or position of the Journal or its management. The information contained in this article should not be considered to be medical advice; patients should consult their own physicians for advice as to their specific medical needs.